Physica D 71 (1994) 146–167
North-Holland

SSDI: 0167-2789(93)E0249-B

PHYSICA D

Peeling the onion of order and chaos in a high-dimensional Hamiltonian system

Kunihiko Kaneko [a,1] and Tetsuro Konishi [b,2]

[a] *Department of Pure and Applied Sciences, College of Arts and Sciences, University of Tokyo, Komaba, Meguro-ku, Tokyo, 153, Japan*

[b] *Department of Physics, School of Science, Nagoya University, Nagoya, 464-01, Japan*

Received 4 May 1993
Revised manuscript received 28 June 1993
Accepted 30 June 1993
Communicated by J.D. Meiss

This paper is dedicated to the memory of Jeff Tennyson, one of the pioneers in chaos and diffusion in Hamiltonian systems with many degrees of freedom. Unfortunately I (K.K.) only had three chances for discussions with him at Berkeley and Los Alamos; however I am grateful that there were such chances at all. I was always impressed by his deep thought. Besides this scientific impression, I somehow felt that though Jeff might have had some difficulties in adapting to his own society, he might have much in common with the Eastern way of thinking and living.

Coexistence of various ordered chaotic states in a Hamiltonian system is studied with the use of a symplectic coupled map lattice. Besides the clustered states for the attractive interaction, a novel chaotic ordered state is found for a system with repulsive interaction, characterized by a dispersed state of particles. The dispersed and clustered states form an onion-like structure in phase space. The degree of order increases towards the center of the onion, while chaos is enhanced at the edge between ordered and random chaotic states. For a longer time scale, orbits itinerate over ordered and random states. The existence of these ordered states leads to anomalous long-time correlation for many quantifiers such as the global diffusion.

1. Introduction

The ordering phenomena in Hamiltonian systems is an interesting and important topic for understanding the origin of chaos and order in nature. A traditional approach in the study of dynamical properties of Hamiltonian systems deals with invariant measure and ergodic properties. Here we focus on non-ergodic and non-stationary aspects of the systems and introduce various interesting phenomena. In a previous paper [1] we have shown that clustered motion is formed even starting from a random phase motion in a class of Hamiltonian systems. In [1] it is shown that the fully developed chaotic ("random") state and clustered motion coexist in the phase space. The clustered motion is also chaotic with a different nature from fully developed ("random") chaos without structure. In the present paper we further explore various forms of order and chaos in a high-dimensional Hamiltonian system. In particular, we investigate more precisely properties of the clustered state and show that the clustered state is not uniform but actually there are many clustered

[1] E-mail address: chaos@tansei.cc.u-tokyo.ac.jp
[2] E-mail address: c42636a@nucc.cc.nagoya-u.ac.jp

states with different degrees of order. We also show that, for repulsive systems, a new ordered chaotic state (called "dispersed order") exists. It will be shown that these clustered states, as well as the dispersed states, form an onion-like structure in the phase space.

Following paper [1], we use a symplectic map system, since it is numerically efficient. Assume that we have N particles on a unit circle and that the state of each particle is defined by its phase (position) $2\pi x(i)$ and its conjugate momentum $p(i)$. Introducing the Hamiltonian

$$H = \sum_{i=1}^{N} p(i)^2 - \frac{K}{(2\pi)^2\sqrt{N-1}} \times \left(\sum_{j \neq i} \cos\{2\pi[x(i) - x(j)]\} \right) \times \sum_{n=-\infty}^{n=\infty} \delta(t-n), \tag{1}$$

the temporal evolution of our model is given by

$$\begin{aligned} &\big(x_n(i), p_n(i)\big) \mapsto \big(x_{n+1}(i), p_{n+1}(i)\big), \\ &\quad i = 1, 2, \ldots, N, \\ &p_{n+1}(i) = p_n(i) + \frac{K}{2\pi\sqrt{N-1}} \times \sum_{j=1}^{N} \sin 2\pi[x_n(j) - x_n(i)], \\ &x_{n+1}(i) = x_n(i) + p_{n+1}(i), \end{aligned} \tag{2}$$

where n represents the time step and i represents the particle index.

When $K > 0$, the interaction term $(K/2\pi\sqrt{N-1}) \sin\{2\pi[x(j) - x(i)]\}$ between two particles i and j is *attractive*, while it is *repulsive* for $K < 0$. The total momentum $\sum_{j=1}^{N} p(j)$ is a constant of motion of the model (2), so that the linear motion of the center of mass is separated from other dynamics. Thus we assume, throughout the paper, that the initial momenta satisfy $\sum_j p_n(j) = 0$ without any loss of generality. The temporal evolution rule is a canonical transformation and the symplectic form is conserved. Thus $2N$-dimensional volume elements are conserved,

$$\mathrm{d}^N p_n \wedge \mathrm{d}^N x_n = \mathrm{d}^N p_{n+1} \wedge \mathrm{d}^N x_{n+1} .$$

As is shown in [1], the model shows clustering of particles for $K > 0$ (attractive) case. Here we will also report a novel ordered state for the repulsive case ($K < 0$). The order is characterized by a dispersed state of particles. Following [1], we evaluate the degree of clustering and dispersion of particles with the following quantity:

$$Z_n \overset{\text{def}}{=} \left| \frac{1}{\sqrt{N}} \sum_{j=1}^{N} \exp[2\pi i x_n(j)] \right|^2 \tag{3}$$

$$\begin{cases} = N & \text{if all } x(j)\text{'s are the same (fully clustered),} \\ \approx 1 & \text{if } x(j)\text{'s are randomly distributed,} \\ = 0 & \text{if } x(j)\text{'s are evenly spaced.} \end{cases} \tag{4}$$

The present paper is organized as follows. In section 2, the repulsive case ($K < 0$) is studied. A novel order with dispersed state of particles is found with the use of the above order parameter Z. The onion structure of many ordered states is clarified in section 3, with the use of Z. These ordered states have a finite lifetime, whose length increases as the orbit goes deeper into the onion structure. The ordered states are also temporally chaotic, whose strength varies by the degree of order, as will be studied in section 4 with the use of Lyapunov spectra. The phase-space structure of many ordered states and the random one are visualized in section 5, by taking a small size system. For a much longer time scale, the orbit shows a switching process between ordered and random states. As will be shown in section 6, this itinerancy over ordered states leads to anomalous behavior of many quantifiers; anomalous

diffusion up to some time scale, stickiness at states without diffusion, as is shown in the diffusion coefficient and order parameter (Z) distributions. The residence time distribution of ordered states also exhibits a power-law behavior. Dependence of the order and randomness on the nonlinearity K is studied in section 7, where global diffusion of momentum is also discussed. Summary and discussions are given in section 8.

2. Repulsive case; dispersed order

In the attractive case ($K > 0$), a clustered state is found when we start from an initial condition with a small momentum variation (e.g., $p(i)$ = random over $[-p_{\rm ini}/2, p_{\rm ini}/2]$; $p_{\rm ini}$ is a small number, say 0.2.), even if the initial phase $x(i)$ is random (see [1]). In that case, most particles take nearby values, forming a cluster. In the present section we show that there is a kind of ordered motion in the repulsive case ($K < 0$), corresponding to the clustered state.

Some timeseries for $K < 0$ are given in fig. 1, starting from an initial condition $x(i)$ = random and $p(i) = 0$ or random. Compared with the time series started from $p(i) = 0$ and $p(i)$ = random, we see that these two time series have a quite different character. A kind of order is seen in the former, but the form of the order is not so clear as in the attractive case just by looking at the figure.

Here Z provides a useful measure to see the existence of order. In the upper half of fig. 1, the corresponding time series of Z_n is plotted. The value is significantly less than unity (expected for a state with random phase).

Through the repulsive interaction, particles

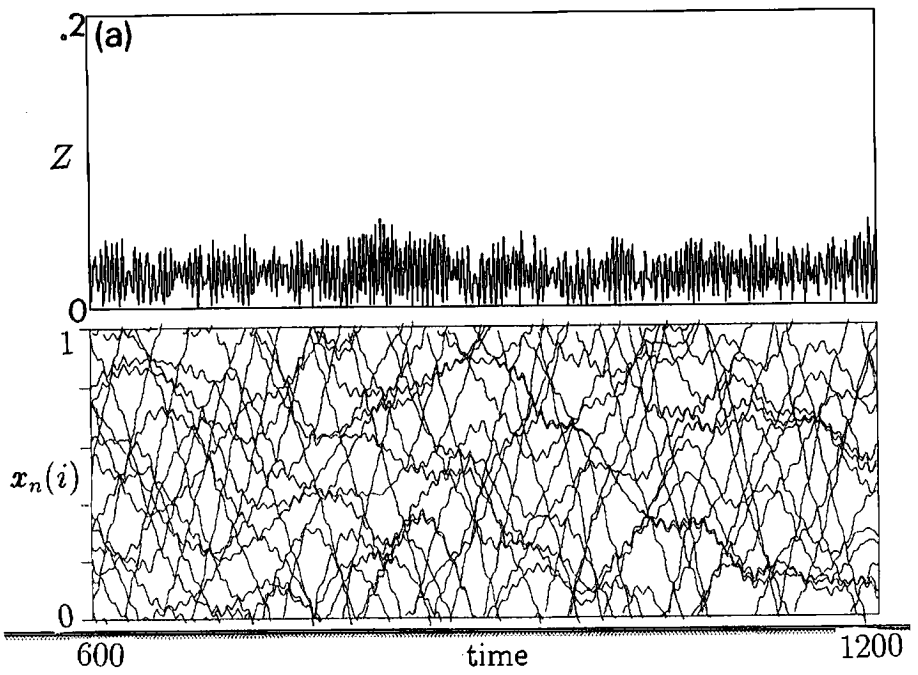

Fig. 1. Typical examples of overlaid timeseries of our model (2), with corresponding timeseries of Z_n. System size $N = 16, K = -0.4$. (a) Dispersed motion: initial condition $x(i)$ = random, $p(i) = 0$. Plotted over the time steps 600–1200. (b) Dispersed motion: initial condition $x(i)$ = random, $p(i)$ = random over $[-0.2, 0.2]$. Plotted over the time steps 600–1200. (c) Random motion: initial condition $x(i)$ = random, $p(i)$ = random over $[-0.8, 0.8]$. Plotted over the time steps 800–1000.

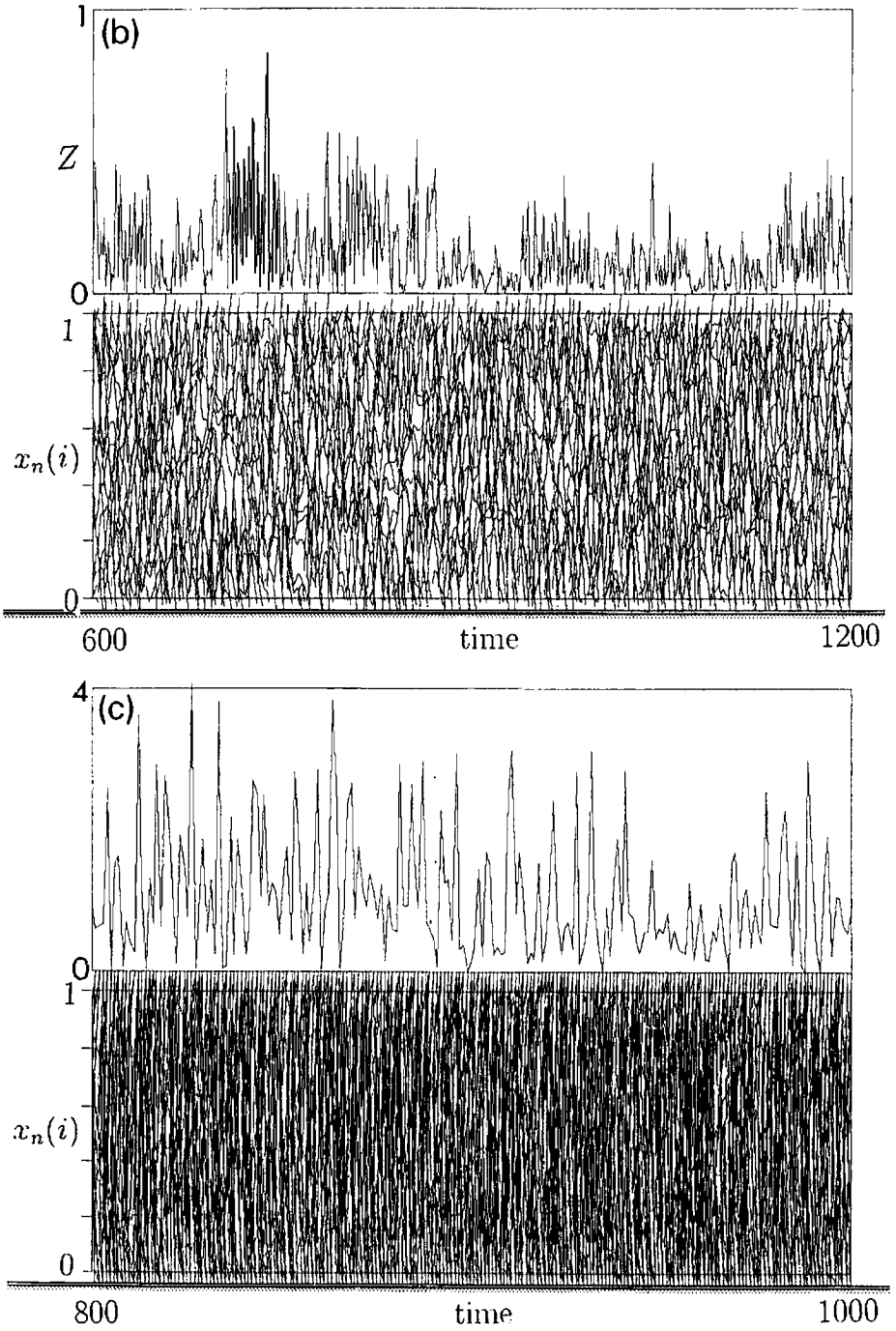

Fig. 1 — continued.

push away each other. A possible limiting case is 'equi-separation',

$$x(i) = \text{const.} + i/N,$$
$$p(i) = \text{const.}, \qquad (5)$$

which is a stationary solution of our model (2) and satisfies $Z = 0$. There are many other stationary states, e.g., $x(i) = c$ for $i =$ odd, $x(i) = c + 1/2$ for $i =$ even, $p(i) = 0$, etc. In the above state in fig. 1, Z has a finite value, but is close to zero. Our state cannot be so regular as the above constant separation case (eq. (5)), but it keeps some order. The above Z values, being much smaller than 1, suggest the existence of some order in the repulsive case, attained by the separation of particles. Here we call this state a *"dispersed" state*.

Thus the value Z gives an index of "order" in our model,

a state is 'clustered' if $Z \gg 1$.

while a state is called 'dispersed' if $Z \ll 1$. (6)

Since clustered and dispersed states have many properties in common, we often name these states together ordered states, here. On the other hand, a fully chaotic state with almost random phases ($Z \approx 1$) here is called "random" state, although its motion cannot be purely random, of course, due to the deterministic temporal evolution of our system.

Simple linear stability analysis yields that the equi-separated stationary state (5) is stable for

$$\frac{N+4}{\sqrt{N-1}}|K| < 8 \ . \qquad (7)$$

We have to note that ordered states are also chaotic, as will be discussed (see also [1]).

3. Coexistence of ordered states in onion

In [1], we treated the system as composed of two different chaotic seas; ordered and random. We see, however, that the ordered state is actually composed of many different states depending on the initial conditions. To see this coexistence, we have used the following one-parameter (p_{ini}) characterization of initial configuration:

$$x(i) = \text{random over}[0, 1] \quad \text{and}$$
$$p(i) = \text{random over}[-p_{\text{ini}}/2, p_{\text{ini}}/2]. \qquad (8)$$

By changing the initial momentum deviation p_{ini}, the nature of ordered states changes successively. In fig. 2, the temporal average value of Z over initial 8000 steps is plotted with the change of initial momentum deviation p_{ini}. We can see the coexistence of ordered states with different levels of order, coded by the value of Z. The ordered state exists only up to some value of p_{ini}. This threshold and the degree of order, of course, depend on K as shown in fig. 2, and will be discussed in section 7.

The average value of Z does not vary significantly within a family of (different random) initial conditions, if the parameter p_{ini} is identical. Hence p_{ini} is a relevant parameter to the degree of order in the system.

To confirm that each ordered state is separated, we have also plotted the time series of Z in fig. 3, where Z_n averaged over 4096 steps is successively plotted. At each time step, the value of Z is distinguishable by states. Thus many ordered states coexist in the phase space as distinct ones.

In two examples in fig. 3, the time series of Z switches from low values to those around 1.0, after a large number of time steps. This switch is a temporal transition from ordered states to the random state. As is discussed in [1], all parts in chaotic sea in the phase space are connected [5,6], including all ordered states and the random state. Thus the ordered states

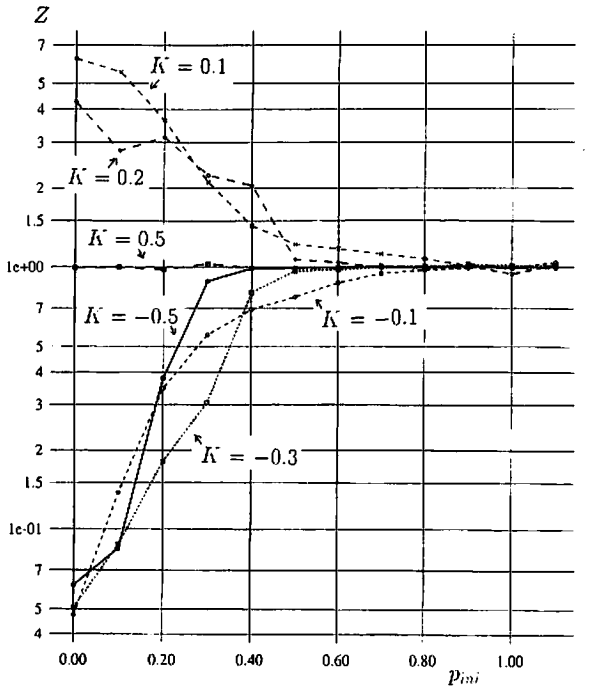

Fig. 2. Average value of Z plotted as a function of p_{ini}. $K = -0.5, -0.3, -0.1, 0.1, 0.2$ and 0.5, $N = 16$. The value Z is obtained from the average of initial 8000 steps, starting from a randomly chosen initial condition parametrized by p_{ini}.

are expected to have *finite* lifetime. Through time evolution an ordered state switches to the random chaotic state distinguished by the Z value around 1.0. (If we wait for a long time, the reverse process is also possible, as will be discussed in section 6.)

In the attractive case, similar separation of the value Z is also seen in corresponding plots as fig. 3. However, the time course of the switching process has a different character between attractive and repulsive cases. In the repulsive case, the switching process progresses rather rapidly, once it sets in. When the switch starts from an ordered state with a very low Z value, the orbit passes, for example, through states with higher Z successively in a short time scale, till it reaches the random state (see fig. 3). In the attractive case, on the other hand, the switching process is rather gradual, as is shown in fig. 4.

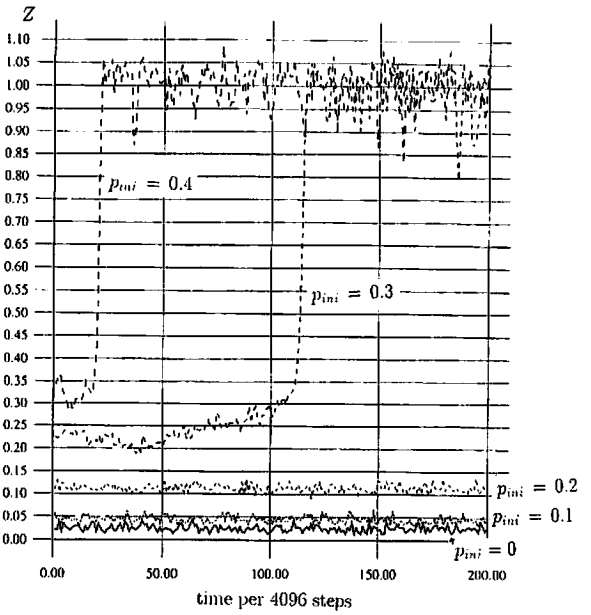

Fig. 3. Time series of Z_n, for different values of p_{ini}. $N = 16$ and $K = -0.4$. Plotted per 4096 time steps. $p_{\mathrm{ini}} = 0$, 0.1, 0.2, 0.3 and 0.4 (from bottom to top).

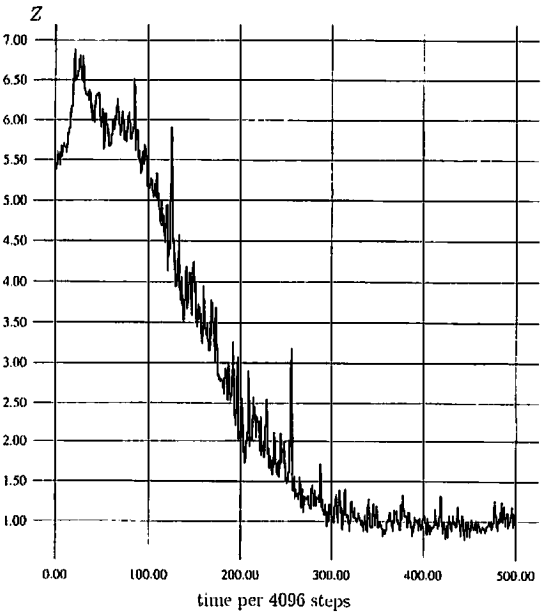

Fig. 4. Time series of Z_n, starting with a random initial condition of $p_{\mathrm{ini}} = 0.1$. $K = 0.15$ and $N = 16$. Plotted per 4096 time steps.

Crossover between ordered and random chaos is a novel type of chaos–chaos transition. As the initial randomness p_{ini} decreases, the duration of such ordered state increases rather rapidly. The increase here might be estimated in a similar manner as given in the Nekhoroshev type argument [7,19], where the transition there is from an apparently regular state near a torus, to a fully chaotic state, while ours is chaos–chaos.

The lifetime of an ordered state depends on its initial condition, which is well represented by the parameter p_{ini} mentioned above. We have plotted the lifetime with the change of p_{ini} in fig. 5. In the repulsive case, the average transient time is roughly fitted with $\exp(\mathrm{const.}/\sqrt{p_{\mathrm{ini}}})$, down to some value of p_{ini}. (We have no reason to expect the divergence at $p_{\mathrm{ini}} = 0$, unless we take a regular initial condition for $x(i)$, for example $x(i) = i/N$ or $x(i) = \mathrm{const.}$) This increase of lifetime is seen clearly in the repulsive case, while the increase with p_{ini} in the attractive case is saturated rather rapidly, and it is not easy to see a simple fitting form. The early saturation (without a simple fitting form) in the attractive case may be related to the gradual collapse of ordered states.

Summing up the section, ordered states coexist in the phase space, like an "onion" structure. This type of onion structure may remind us of that supported by KAM tori and islands, as are often seen in pendula or the standard map [3]. In contrast with these examples from low degrees of freedom, our "onion" consists of chaos, not of tori.

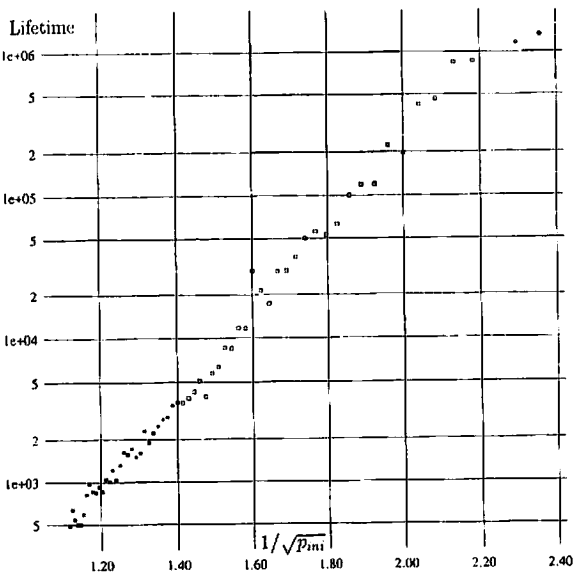

Fig. 5. Semilog plot of the average lifetime of ordered state versus $1/\sqrt{p_{\mathrm{ini}}}$. The average is taken from 80 samples (for $0.5 < p_{\mathrm{ini}} < 0.8$) with different random configuration with given p_{ini}, and from 40 samples for $0.2 < p_{\mathrm{ini}} < 0.5$, and from 20 samples for $0.15 < p_{\mathrm{ini}} < 0.2$. The lifetime is estimated as the time step at which Z_n exceeds 0.99 for the first time. $K = -0.4$ and $N = 16$.

4. Chaos in ordered states

As is noted in [1], the dynamics of the ordered state is also chaotic. Here we study how the strength of chaos varies with the degree of order in the clustered/dispersed states. For this purpose, we use the Lyapunov spectrum, a characteristic of asymptotic orbital instability of dynamical systems. It is a set of real numbers with $2N$ elements $\{\lambda_1, \ldots, \lambda_{2N}\}$ and defined from an eigenvalue spectrum of the squared Jacobi matrix,

$$J(t) \stackrel{\mathrm{def}}{=} \frac{\partial (\boldsymbol{p}(t), \boldsymbol{x}(t))}{\partial (\boldsymbol{p}(0), \boldsymbol{x}(0))}, \tag{9}$$

$$\{\mathrm{e}^{2\lambda_1 t}, \ldots, \mathrm{e}^{2\lambda_{2N} t}\} = \text{eigenvalue spectrum of } {}^{t}J(t)\,J(t) \text{ as } t \to \infty. \tag{10}$$

Note that, with this definition, a Lyapunov spectrum can depend on the initial condition. For actual computation of exponents we use the standard method [21,22] with Gram–Schmidt orthonormalization.

We arrange the exponents as decreasing order $\lambda_1 \geq \lambda_2 \geq \ldots \geq \lambda_{2N}$. Since $\lambda_{2N+1-i} = -\lambda_i$ due to the symplectic condition, only the bigger half of the whole spectrum is necessary. Some examples of Lyapunov spectra are plotted in fig. 6, where

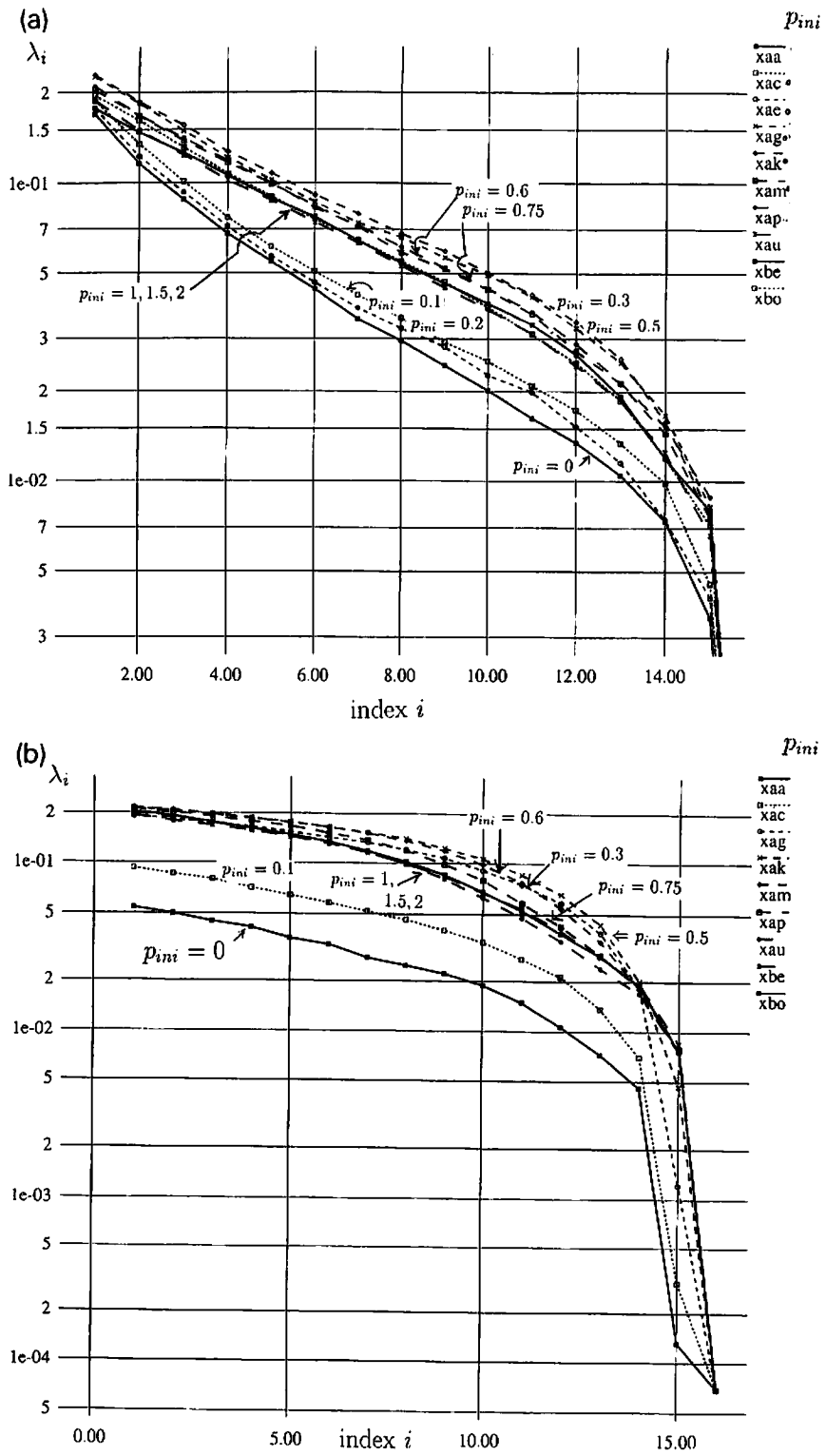

Fig. 6. Lyapunov spectra λ_i for the model (2) with $N = 16$. Spectra are obtained from the average over initial 10000 steps. (a) $K = -0.2$. Spectra from $p_{\text{ini}} = 0, 0.1, 0.3, 0.5, 0.6, 0.75, 1, 1.5$ and 2 are overlaid. (b) $K = 0.2$. Spectra from $p_{\text{ini}} = 0, 0.1, 0.2, 0.3, 0.5, 0.6, 0.75, 1, 1.5$ and 2 are overlaid.

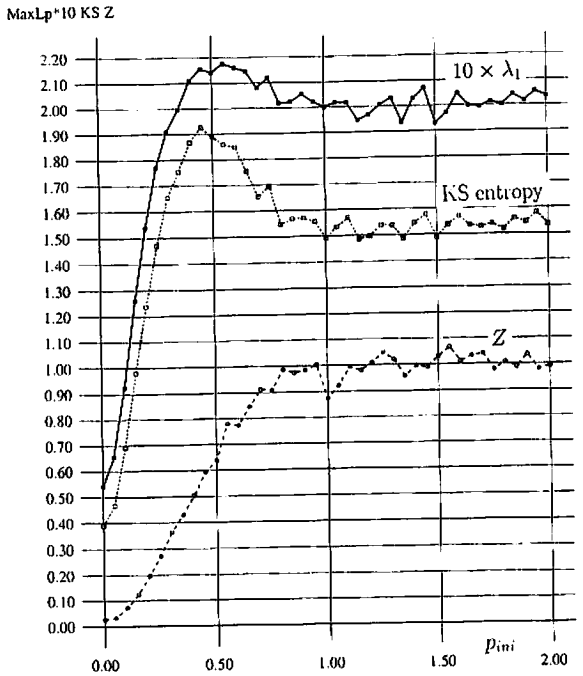

Fig. 7. The maximal Lyapunov exponent (thick line: multiplied by 10 times for the convenience of scale), KS entropy (dotted line), and the average value of Z (broken line) are plotted as a function of initial p_{ini}. $N = 16$. Obtained from the average over initial 10000 steps. $K = 0.2$ (KS entropy is multiplied by 5 for scaling).

initial conditions are taken as eq. (8). We note that all the exponents are much lower for $p_{\mathrm{ini}} = 0$ than other cases. As p_{ini} is increased, the exponents are shifted upwards, up to some value of p_{ini}, and then decrease again to approach the spectra for the random state. To see this p_{ini}-dependence clearly we have plotted the maximal Lyapunov exponent and Kolmogorov–Sinai (KS) entropy (estimated by $\sum_{j=1}^{N} \lambda_j$) with the change of p_{ini} in fig. 7. The enhancement of chaos at the border between random and ordered chaos is found both in clustered and dispersed cases.

In the course of collapse of clustered states, chaos is enhanced as is shown in fig. 8, where we have computed the local Lyapunov spectrum and Z, averaged over a given (finite) time steps ($=4096$ in the figure). From the computation, we have obtained the local Lyapunov exponents

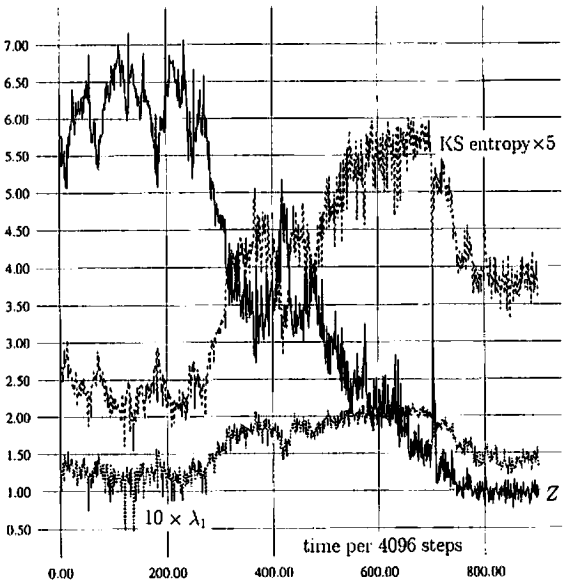

Fig. 8. Temporal evolution of local Lyapunov exponents. The maximal Lyapunov exponent (thick line: multiplied by 10 times for the convenience of scale), KS entropy (dotted line: multiplied by 5 times), and the average value of Z (broken line) are plotted as a function of time per 4096 steps. All the values are the average for 4096 time steps at each time. $K = 0.15$, $p_{\mathrm{ini}} = 0.1$, and $N = 16$.

at each time step, as the short-time average of the exponents. As is shown in fig. 8, both the maximal Lyapunov exponent and KS entropy are gradually enhanced as Z is decreased (that is, as the orbit goes to the outer part of the onion structure). With increasing time, the local Lyapunov exponent and KS entropy take maximal values just before Z approaches unity. Reaching the random chaotic state, the Lyapunov exponents are again decreased to settle down to a constant value. The intermediate enhancement at the collapse is not clearly seen in the repulsive case, since the orbit passes through the outer part of the onion within a short time scale.

Chaos in a kicked system as ours often exhibits the diffusion in momentum space, as has been intensively studied in the standard map. Indeed the random state in our system shows diffusive motion, as is studied in [17] and in section 6. Is this true for chaos in ordered states?

For the study of local diffusion in phase space,

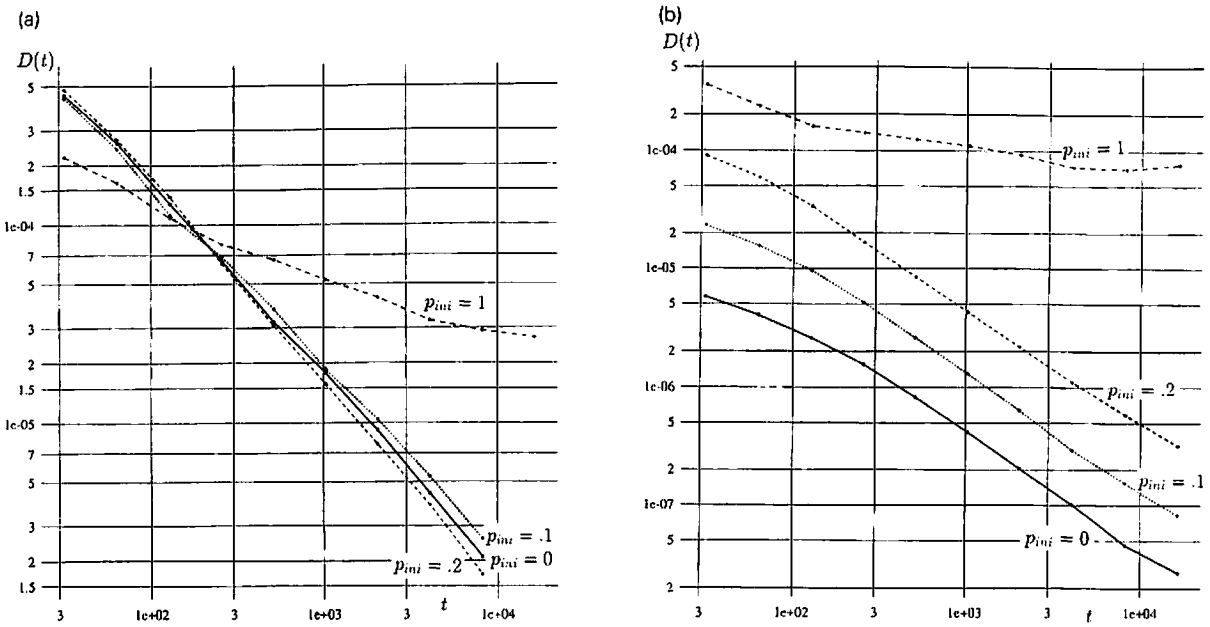

Fig. 9. Local diffusion coefficient $D(t)$ for ordered states; Obtained with 10–100 sequential sampling, starting from the initial condition with $N = 16$, $p_{\mathrm{ini}} = 0, 0.1, 0.2$ and 1. (a) $K = 0.2$ and (b) $K = -0.2$

it is often useful to introduce the following local diffusion coefficient, defined by

$$D(t) \equiv \left\langle \frac{1}{t}\frac{1}{N}\sum_i [p_{n+t}(i) - p_n(i)]^2 \right\rangle, \qquad (11)$$

where the bracket $\langle \cdots \rangle$ represents the long-time average [17], i.e. average over many n's.

If the diffusion in the phase space is normal, there exists a constant $D_\infty \equiv \lim_{t\to\infty} D(t) > 0$. If the diffusion is fractional, $D(t) = t^{-\delta}$, with some positive exponent $\delta < 1$, which characterizes the stickiness of such diffusion. If the orbit is localized without any global diffusion, $D(t) \propto 1/t$. For the ordered state, $D(t) \propto 1/t$ over all time steps within its lifetime (see fig. 9). This $1/t$ decrease is in contrast with the diffusion in the random chaotic state (plotted in fig. 9, for reference, by taking the initial condition $p_{\mathrm{ini}} = 1$). Thus there is no global diffusion in the momentum space for the ordered state, although the motion is chaotic. Indeed, the localization of orbits is necessary to have the onion structure, where the value of Z remains distinct by initial conditions.

For the attractive case, $D(t)$ for the clustered state is larger than that for the random state, if t is small. The momentum oscillates with a larger amplitude for the clustered state, but does not show global diffusion. On the other hand, $D(t)$ (even for small t) is much smaller in the dispersed state. It monotonically increases with p_{ini} up to the random state.

5. Structure in the phase space

To understand the onion structure of chaos and order, it is essential to explore the structure in the phase space in detail. Since the "anatomy" of high-dimensional phase space is difficult to visualize, we study a rather low-dimensional case here, by restricting the number of particles to 4. (Due to the conservation law, the phase space is 3×2 dimension.)

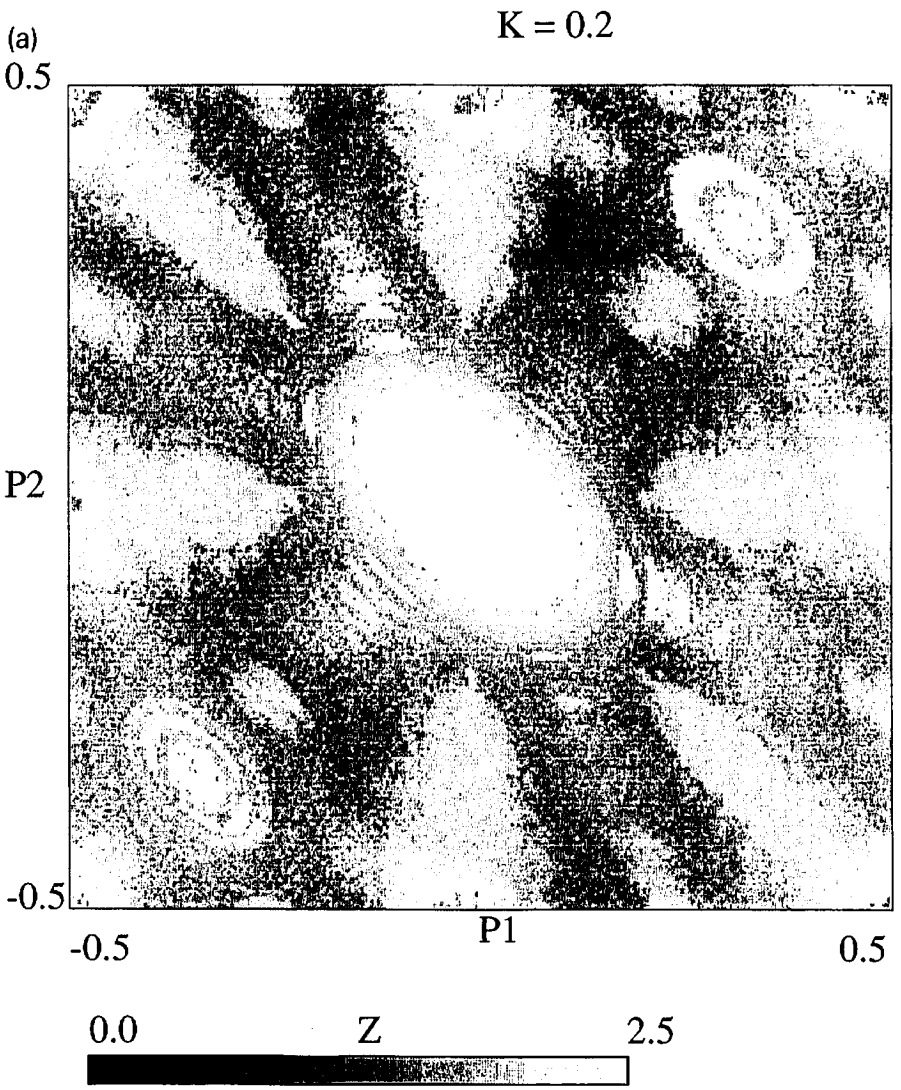

Fig. 10. A 2-dimensional surface of section $(p(1), p(2))$ of the model (2). Number of particles is $N = 4$, and coupling constants are (a) $K = -0.05$, (b) $K = 0.05$, (c) $K = 0.2$. In the $(4 \times 2 =)$ 8-dimensional phase space, the section is taken by setting the following 6 constraints; (b) $x(1) = -0.075 = -x(4)$, $x(2) = -0.025 = -x(3)$, $p(3) = 0$, and $p(4) = -p(1) - p(2)$ so that the center of mass is fixed; $\sum_1^4 x(i) = \sum_1^4 p(i) = 0$. The last two constraints come from conservation of the total momentum so that the points shown in the figure have the same value of total momentum, which is a conserved quantity. We set 256×256 (for $K = 0.05$) or 512×512 (for $K = -0.05, 0.2$) lattice points on the 2-dimensional section, which are taken as initial conditions for the time evolution. The value of Z averaged over 10000 steps are plotted with a gray scale corresponding to the initial condition of $(p(1), p(2))$.

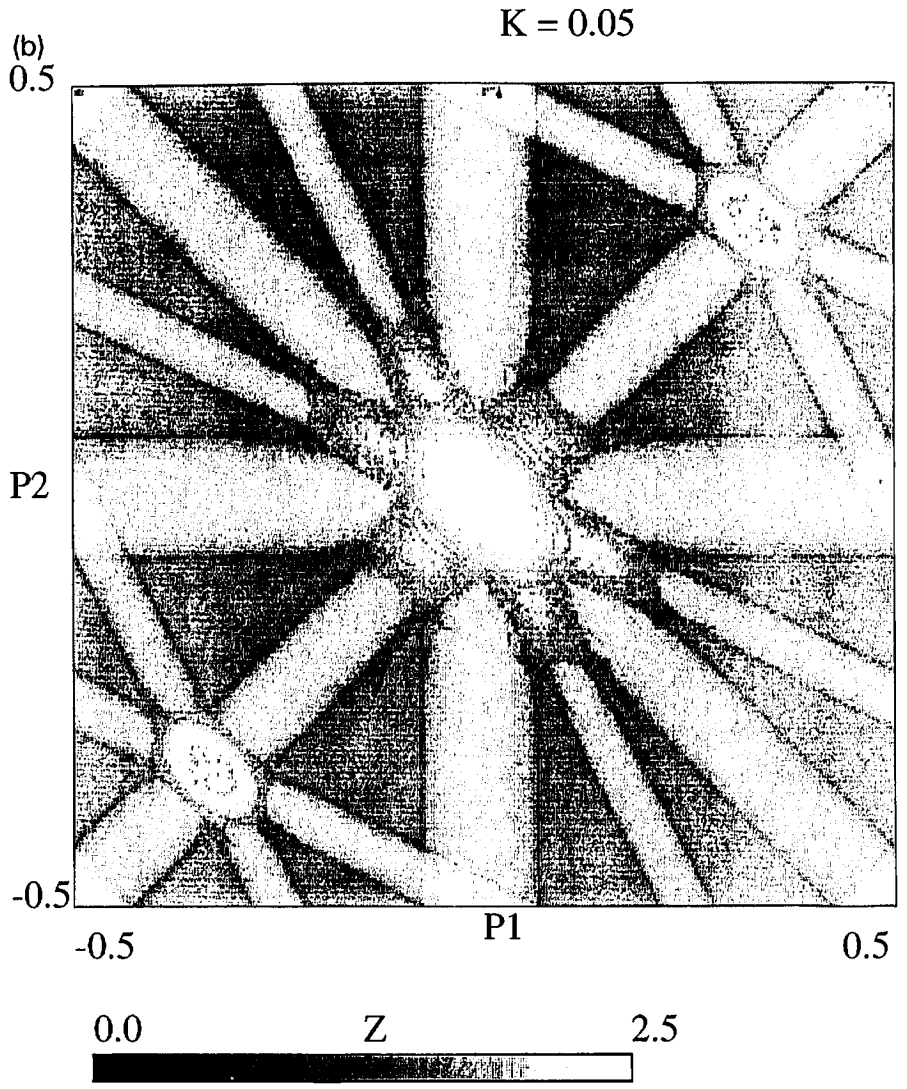

From the 6-dimensional phase space, we take a two-dimensional slice for visualization. Here we sample the dynamics of initial conditions of 512×512 points in $(p(1), p(2))$-space by fixing $x(1), x(2), x(3)$ and $p(3)$. In addition, $x(4)$ and $p(4)$ are determined from the constraints $\sum_{j=1}^{4} p(j) = 0$ and $\sum_{j=1}^{4} x(j) = 0$.

In fig. 10, Z values are plotted, obtained from the average over 256 steps starting from the corresponding phase space points. Corresponding plots of the maximal Lyapunov exponent averaged over 256 time steps are given in fig. 11.

For the attractive case, the core of the onion is seen around $(p(1), p(2)) \approx (0, 0)$. The value Z increases monotonically as the point approaches the origin. We can see a threshold for the momenta below which the ordered states exist. Besides this expected structure, we have also seen regions corresponding to ordered states near a two-clustered state with 1:3 (around $(p(1) = p(2) = p(4)) \approx (\pm 1/3, \pm 1/3)$). From the edge of the onion, broad resonant structures are emit-

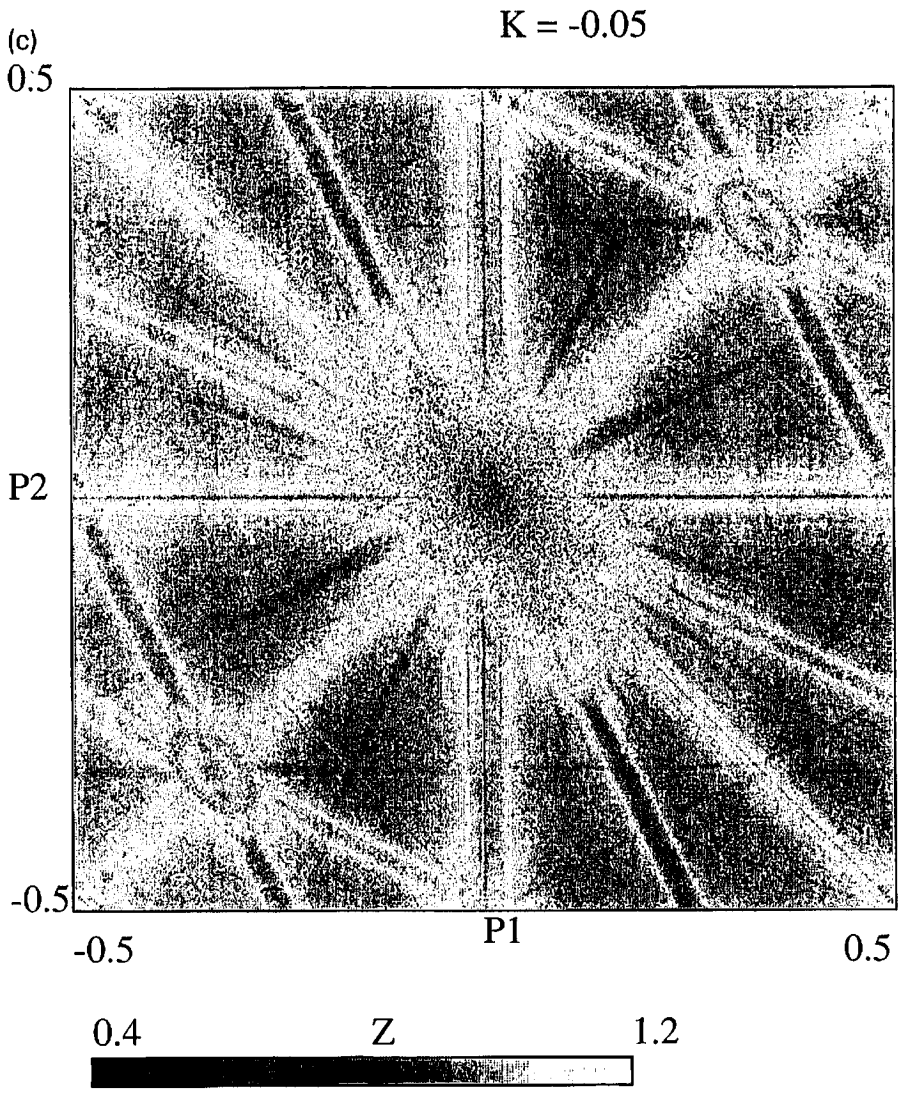

Fig. 10—continued.

ted where Z values are rather low, and the Lyapunov exponent is rather high. This structure supports the enhancement of chaos at the edge between order and chaos.

For the repulsive case, we have again observed the onion structures around $(p(1),p(2)) \approx (0,0)$, and the satellite structure (around $(p(1),p(2)) \approx (\pm 1/3, \pm 1/3)$). The onion structure, however, is not smoothly constructed as in the attractive case. The Z value changes in the momentum space not gradually, but it sensitively depends on the initial condition even around $(p(1),p(2)) \approx (0,0)$ ("chopped onion" structure). This may be the reason why the switching from dispersed to random states are rapid in the repulsive case. Furthermore, some resonant structures are clearly visible satisfying the conditions $p(1) = \pm p(2)$, $p(1) = \pm 2p(2)$, $p(2) = \pm 2p(1)$, and so on (see also [13] for the resonant structure in higher dimensional phase space, as well as the pioneering work [31]).

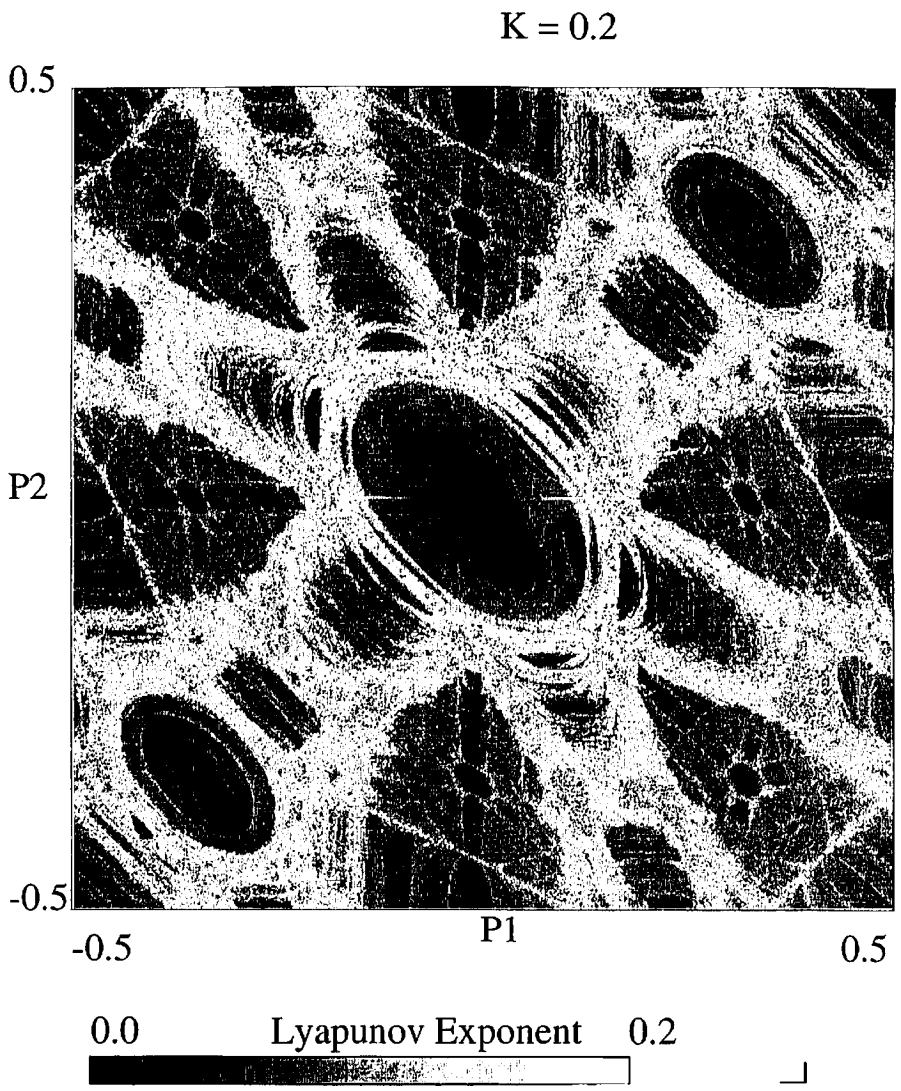

Fig. 11. Maximal Lyapunov exponents are plotted depending on the initial condition. The same slice as fig. 10 is used. Starting from the initial condition corresponding to the point in the slice, we have measured the maximal Lyapunov exponent averaged only over 256 time steps, and they are plotted with the gray scale. $K = 0.2$.

A problem in the anatomy in the present section is that the size ($N = 4$) may be too small. This problem seems to be more serious in the repulsive case, since particles can often split into two groups with two elements or with one and three elements; such separation can lead to a larger value of Z than 1, and bring about some difficulty in the distinction of ordered ($Z < 1$) and random states.

The problem for the small size is also seen in the chopped onion structure, which is in apparent contradiction with the smooth onion picture in section 3. We believe that the smoothness is attained with the increase of size (even in the repulsive case), where many degrees of freedom may smear out fine structures in the phase space.

6. Order within chaos

The existence of ordered states affects the long time behavior of the (random) chaotic motion. The orbit visits many ordered states during the long term evolution. Switching between the random and ordered states can occur. How do the remaining ordered states affect the long-term statistical behavior of the dynamics? To address this question, we have studied the behavior of (1) the local diffusion coefficient $D(t)$, (2) the local diffusion distribution, (3) the residence time distribution at ordered state, and (4) the distribution of the local order parameter (Z).

6.1. *Local diffusion coefficient $D(t)$*

$D(t)$ is a good characteristic to search for order within chaos. As shown in fig. 12, $D(t)$ shows an anomalous power law decay $D(t) \propto t^{-\delta}$ up to some crossover time. This remnance of sticky behavior up to a large time suggests the long-time residence of the orbit near an ordered state.

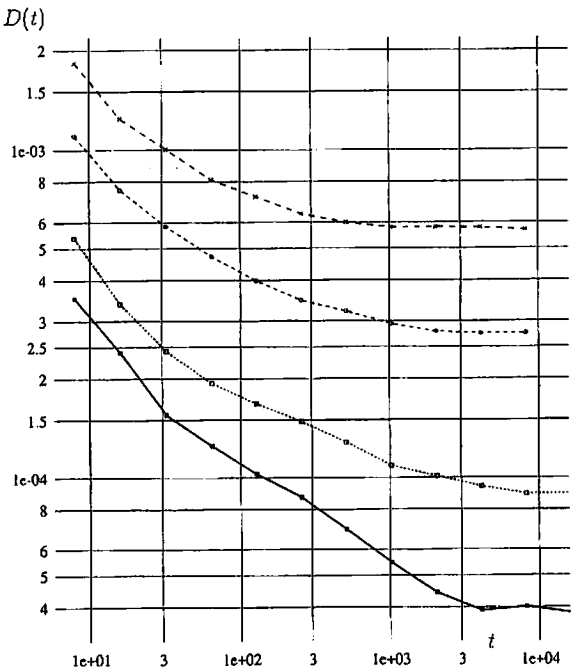

Fig. 12. Local diffusion coefficient for the random state; Obtained with the average over 200 sequential sets of data (totally from 200 × t steps), starting from a random initial condition with $p_{\mathrm{ini}} = 1$. $N = 40$. Log–log plot. $K = 0.4, 0.3, 0.2, 0.15$ from top to bottom.

6.2. *Local diffusion distribution*

As another direct way to see the sign of ordered states, we have measured the distribution $P(d)$ of short time diffusion coefficient for each particle, $d_i(t) = [p_{n+t}(i) - p_n(i)]^2$. The distribution $P(d)$ is given in fig. 13 for ordered and random states. The distribution is fitted in the following form:

$$P(d) \approx \begin{cases} d^{-\alpha}, & \text{for small } d, \\ \exp(-\text{const.} \times d), & \text{for large } d. \end{cases} \quad (12)$$

For large $|K|$ (e.g., $|K| > 0.7$), the exponent α agrees with $1/2$. The value $1/2$ is easily explained by the central limit theorem: If we assume that the position $x(i)$ of particles are independent random numbers, we can expect that the distribution of the force term $\sum_{j=1}^{N} \sin\{2\pi[x_n(j) - x_n(i)]\}$ obeys the Gaussian distribution. The (average of the) square of this variable gives the local diffusion $d_i(t)$. If a variable z obeys the Gaussian distribution, the variable $y = z^2$ obeys the distribution $y^{-1/2}\exp(-\text{const.} \times y)$, thus leading to the above behavior.

On the other hand, the exponent α is rather close to 1 for small K where ordered states exist in the phase space. The value $\alpha \approx 1$ ($> 1/2$) suggests the stickiness to states near $D \approx 0$. As is shown in the previous section, there is no diffusion in the phase space for the ordered states. Thus the enhancement of the exponent α means that the orbits are frequently stuck to ordered states.

6.3. *Residence time distribution*

To see the residence at ordered states more explicitly, we have measured the residence time distribution at ordered states. Take a long time series and decompose the time interval into

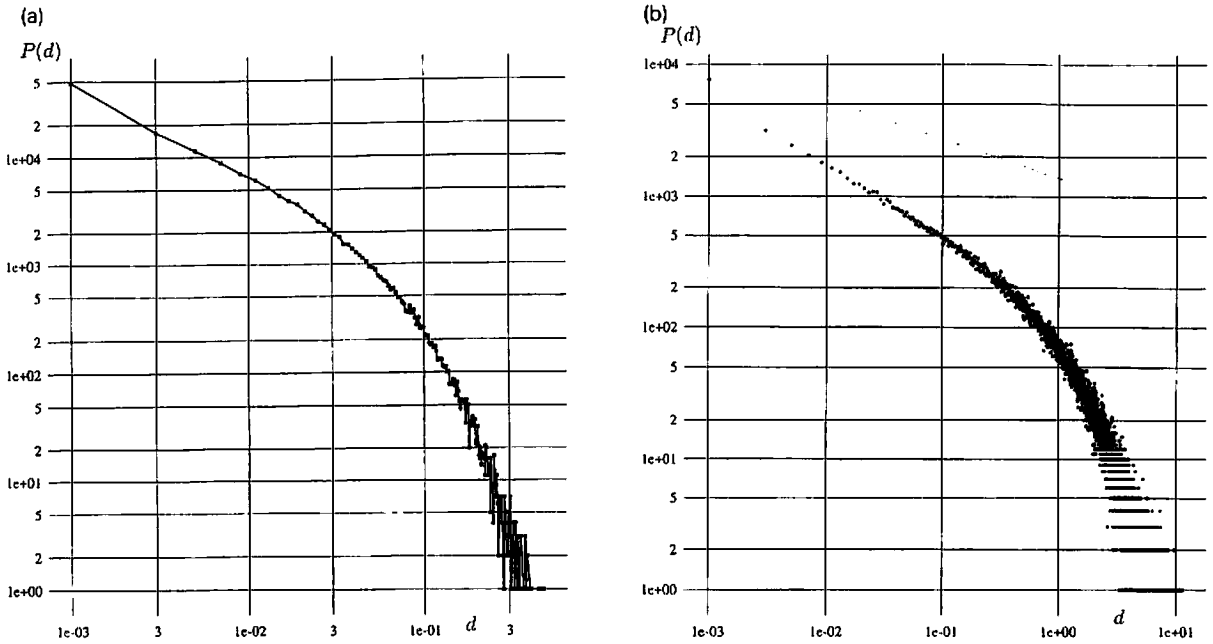

Fig. 13. Distribution of diffusion coefficient $d(i) = [p_{n+\tau}(i) - p_n(i)]^2$. The average time τ is chosen to be 512. $N = 16$ and $p_{\text{ini}} = 1$. Sampled over 10000 times per τ steps. Log–log plots. (a) $K = 0.15$ and (b) $K = 0.8$.

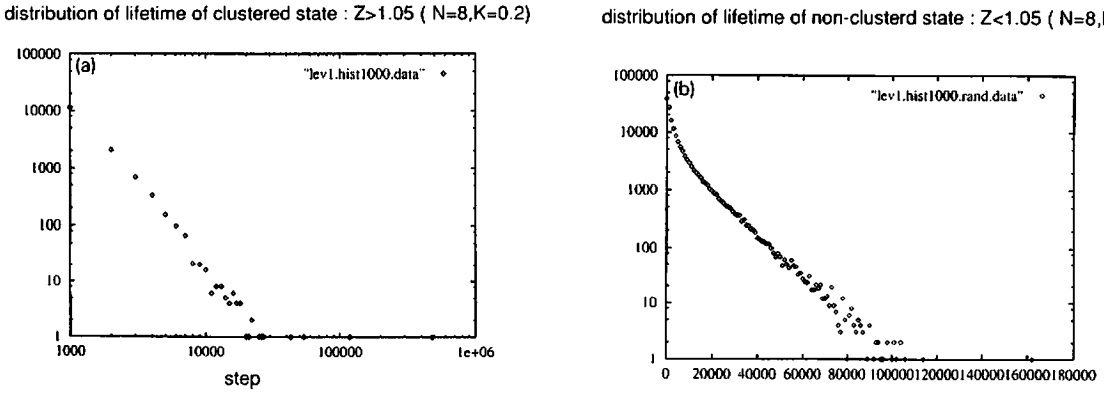

Fig. 14. Residence time distribution at ordered and random states (a) for ordered ($Z > 1.05$), (b) for random ($Z < 1.05$) states. $N = 8$ and $K = 0.2$. Total length of time series = 10^9. Note that the distributions (a) and (b) are independent of each other.

segments of 'clustered parts' and 'non-clustered parts' by properly choosing a threshold value Z, say 1.05 (we study the attractive case here). The length of each segment represents a residence time at the clustered or non-clustered state. From the set of segments we can see the distribution of residence times as seen in fig. 14.

Indeed the residence time distribution at ordered states obeys the power law distribution $t^{-c}, c \sim 3.4$, which means that no characteristic time scale exists in this region. For the random state we have $\exp(-c't)$ distribution, implying uncorrelated motion of particles. For the ordered state the exponent c is greater than 1 and the average residence time is finite. Thus the temporal switching between the ordered and random states continues forever.

The above difference between the two distributions means that the switch between the two states is quite asymmetric. From random to ordered states the switch occurs through a kind of random trap to holes, while the reverse switch is rather gradual. The orbit slowly departs from the ordered states. This type of asymmetric switch is commonly observed in the chaotic itinerancy [27,28].

6.4. *Distribution of local order parameter Z*

Another characteristic is a distribution of the order parameter Z over the phase space, where Z is calculated as finite time average. We have measured the distribution of Z averaged over a given time step τ in fig. 15. The distribution has a peak around $Z \approx 1$, with exponential tails to both sides. The tail extends deeper to $Z < 1$ (for the repulsive case) or $Z > 1$ (for the attractive case), respectively. The inner part of the "onion" structure is less frequently visited.

From the distribution of Z, we have also studied the decrease of its variance with the increase of sampling time τ. It is found that the variance decreases with the coarse-grained time τ as $\mathrm{Var}(Z) \approx \tau^{-1}$ for large K, in accordance with the central limit theorem, while it decays as $\tau^{-1/2}$ for small K. This slow decay again suggests the sticky motion to ordered states.

The scaling here corresponds to large deviation analysis [23]. The power law distribution in the residence time often leads to the anomalous scaling in the large deviation. Indeed Kikuchi and Aizawa [24] have shown a relationship between the power of residence time and the scaling for the variance, by taking a two-state semi-Markovian process. According to our numerical simulation, however, the relationship between c in subsection 6.3 and the exponent here does not quantitatively agree with their theory. Following their theory, the central limit theorem with usual scaling ($\propto \tau^{-1}$) is valid if $c > 2$ (as in our case), in contrast with our anomalous scaling with τ. We believe that this discrepancy comes from the fact that our ordered states are not single. An infinite-state (rather than a two-state) semi-Markovian process must be necessary for a quantitative analysis.

Results of the present section are summarized in table 1.

7. Parameter dependence and global diffusion

As our model (2) is integrable for $K = 0$, the parameter K can be regarded as the magnitude of perturbation for the integrable model. As the perturbation K is changed, the degree of order in the ordered state varies, as well as the volume of the phase space supporting the ordered states. In fig. 16, we have plotted the average value of Z over initial 8000 steps, starting from the initial conditions $p_{\mathrm{ini}} = 0, 0.1, 0.2, \ldots, 1.1$.

As is shown in fig. 16, ordered states disappear as $|K|$ gets larger. We note that the mechanism of disappearance is different between attractive and repulsive cases. In the attractive case, the value Z for clustered states decreases towards 1, the value for the random state, as K is increased (see fig. 16). In other words, the "order" in a clustered state decreases with K till the state is absorbed into the random chaotic state. In the

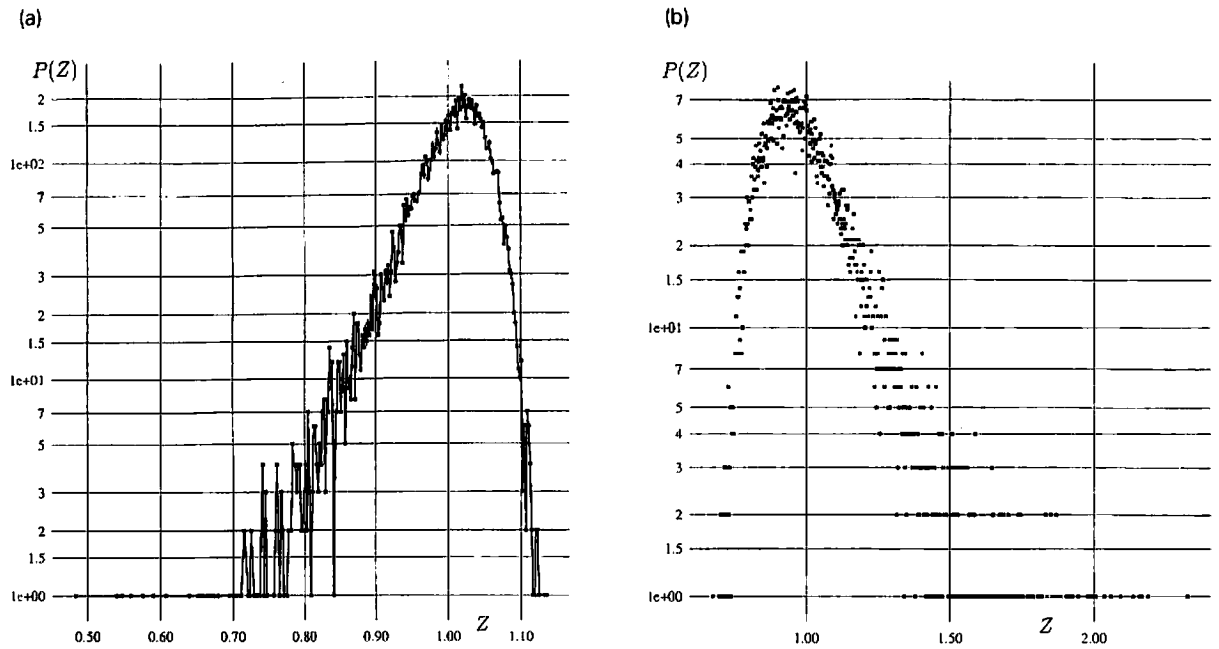

Fig. 15. Distribution of Z averaged over τ time steps. $N = 16$ and $p_{\text{ini}} = 1$. Sampled over 10000 times per τ steps. (a) $K = -0.4$ with $\tau = 2048$ and (b) $K = 0.15$ with $\tau = 1024$.

Table 1
The anomalous behaviour for several quantifiers (h.n. = high nonlinearity; large K).

Quantifiers	Anomalous behavior	cf.
$D(t)$	crossover from $t^{-\delta}$ to D_∞	D_∞ for h.n.
local diffusion distribution $P(d)$	d^{-1}	$d^{-1/2}$ for h.n.
residence time distribution $P(t)$	$t^{-3.4}$ for ordered states	$\exp(-t)$ for random states
$\text{Var}(\tau)$; variance of local Z	$\tau^{-1/2}$	τ^{-1} for h.n.

repulsive case, there remains a large gap in Z between the dispersed and random states (see fig. 16). Thus the ordered states still remain as a structure even if $|K|$ is increased. Instead, the lifetime for these dispersed states decreases with $|K|$ till, for large $|K|$, it is too short for the states to be observed as a temporally stable one.

Of course the long-term behavior of chaos varies with the nonlinearity K. The diffusion constant D, estimated as $\lim_{t\to\infty} D(t)$ is plotted in fig. 17.

First we have to recall that the coupling constant K is scaled by $\sqrt{N-1}$ so that the model is expected to show extensive behavior in a strongly chaotic regime $K \gtrsim 1$. In the strongly chaotic regime, correlation among particles is negligible. Thus the force terms $(2\pi\sqrt{N-1})^{-1} K \sum_{j=1}^{N} \sin\{2\pi[x_t(j) - x_t(i)]\}$ can be approximated by stochastic variables independent of the system size N. This approximation leads to the proportionality of diffusion coefficient to K^2, which is numerically confirmed for $K \gtrsim 1$ [2]. Due to the scale factor of $\sqrt{N-1}$ in front of K, the diffusion constant approaches a size-independent value as N is increased (see fig. 17).

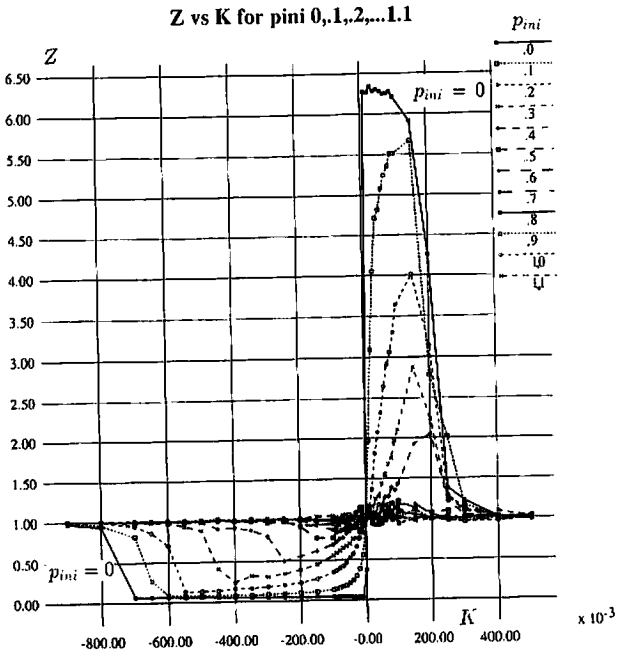

Fig. 16. The average value of Z over 8000 steps, with the change of K, starting from a random initial condition with $p_{\mathrm{ini}} = 0, 0.1, 0.2, ..., 1.1$, $N = 16$.

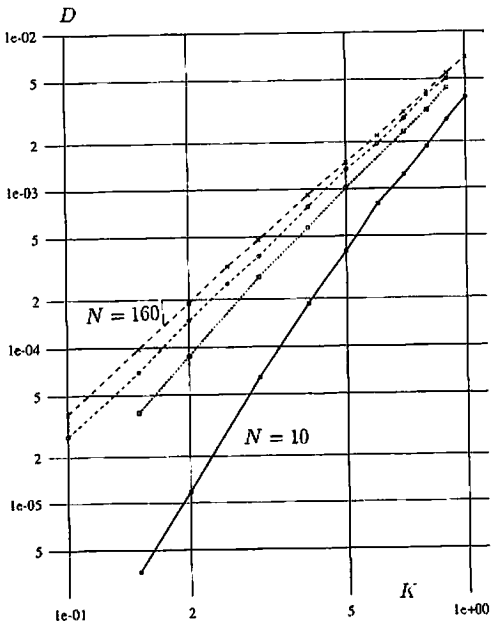

Fig. 17. The diffusion constant D vs K. D is estimated by the asymptotic value of $D(t)$ converging with the increase of t, from the plot of $D(t)$ corresponding to fig. 12. Obtained with 200 sequential average, starting from a random initial condition with $p_{\mathrm{ini}} = 1$, $N = 10, 40, 80$ and 160. Log–log plot.

In a smaller K regime, the diffusion constant D increases as K^{σ} increases with the exponent σ different from 2. This power slowly decreases with the size N, as shown in fig. 17. The estimated exponent σ is given in table 2. We note here that this is not a Nekhoroshev-type dependence $D \propto \exp(cK^{\alpha})$ [4], which is expected to hold for nearly integrable systems. The fractional power law dependence, which is also numerically observed in another model [2], reminds one of "Fast Arnold Diffusion" for the intermediate perturbation strength (see Chirikov and Vecheslavov [25]). As the system size gets increased, however, the exponent α here is closer to 2, the value expected by random phase approximation, whereas the fast Arnold diffusion theory predicts $\alpha \sim 6.6$. It may be necessary to study a regime with smaller K for such a large system ($N > 40$).

Table 2
$D \propto K^{\sigma}$.

Size N	10	40	80	160
Exponent σ	4.1	2.75	2.44	2.34

8. Summary and discussions

In this paper we have discovered a new type of ordered states in *Hamiltonian* systems. This ordered state, called the "dispersed order", appears in a system with repulsive interaction. It is sustained dynamically as in the clustered state previously discovered. In the dispersed order, particles are scattered in a well-organized manner. The order is characterized by the parameter $Z_n = (1/N)|\sum_j \exp[2\pi i x_n(j)]|^2$. For dispersed ordered states, the average of Z_n takes much smaller values than unity.

The discovery of repulsive order in our state

reminds us of the Alder transition or Wigner lattice, where spatial order appears through repulsive interaction between particles. In contrast with these established examples, our "dispersed order" state in the repulsive model is more subtle, neither with a clear periodic structure in space, nor with a static order. The "dispersed order" does not form a regular lattice as in the Alder transition but rather resembles a liquid state. Although our example here has a global interaction among particles, it is rather straightforward to introduce a model with a short-ranged interaction that shows a repulsive order as in the present example. These examples suggest that the order formation in a Hamiltonian system with repulsive interaction is rather common in nature.

The order in the repulsive interaction is also seen in dissipative systems. Indeed we have found a clustering state (with 3 clusters) sustained by the repulsion of each particle, for a globally coupled (dissipative) circle map [28]. Such a clustered state has a different nature from the attractive case.

Both the clustered and dispersed states have many features in common as ordered states. These states in our Hamiltonian system form an onion-like structure in the phase space. The degree of order decreases as the initial momentum variance is increased, till the "random" chaotic sea replaces the ordered state beyond some threshold for the momentum variance. The ordered states also show chaotic behavior, although the orbits do not show global diffusion in the phase space. This localization of orbits gives a basis for the onion structure. It is found that chaos is enhanced at the edge between the ordered and random states. Orbital instability is strongest at the transition from ordered to random states.

Coexistence of ordered and random states in Hamiltonian systems is already reported in [1]. Here we have shown that the ordered state is actually a union of states with various degrees of order. The coexistence of many ordered states is important, particularly when we think of quantum versions of the models, since the wave function spreads over the various ordered and non-ordered states in the phase space.

Although the clustered and dispersed states (for attractive and repulsive interactions respectively) have many chaotic features in common, there are some differences between the two, as is summarized in table 3. So far it is not clear how these differences are interrelated, and if they can be explained from the phase space structure.

Since all chaotic orbits are connected for a Hamiltonian system with many degrees of freedom, an ordered state has a finite life time before it is switched into the random state. Conversely, an orbit in the random chaotic state visits ordered states. The existence of the ordered states bring about anomalous long-time behavior in dynamics. Local diffusion (up to some crossover time) and the residence time distribution at ordered states show anomalous power-law behavior, as well as the distributions of local diffusion coefficients and of the order parameter Z. The above behaviors are the manifestation of the existence of long-time correlation. Such power-law correlation implies the $1/f^{\alpha}$ spectra for the Fourier transformation of autocorrelation of dynamic variables ($\alpha = 2-\delta$, see [17]). We note that these long-time correlations always appear when the coupling K is small. In other words, we can expect that long-time correlation generally appears in a Hamiltonian system (which is also true of a continuous-time case; see the later argument). Thus we can expect that $1/f^{\alpha}$ behavior generally appears in a high-dimensional Hamiltonian dynamical system. This explains at least some of the origins of $1/f^{\alpha}$ spectrum in nature, in particular in the fluctuation around equilibrium states [26]. The exponent α indeed approaches 1 as the coupling K is decreased [17].

The lifetime of the clustered and dispersed states increases with $|K| \to 0$. Since a proper limit with $|K| \to 0$ gives a flow system of a time-independent Hamiltonian, we can expect that clustered and dispersed order are more fre-

Table 3
Differences between clustered and dispersed states for attractive and repulsive interactions.

Interaction	Attractive ($K > 0$)	Repulsive ($K < 0$)
Z	$\gg 1$	$\ll 1$
collapse of order with time	gradual	sudden
behavior of lifetime with $p_{\mathrm{ini}} \to 0$	early suppression	increase with $\exp(-p_{\mathrm{ini}}^{-1/2})$
collapse with the increase of $\lvert K \rvert$	merge into random states	lifetime goes to 0
$D(t)$ for small t	larger than the random state	smaller than the random state
phase space structure for $N = 4$	smooth onion	non-smooth

quently observed in a Hamiltonian system with continuous time. In the continuum limit, p_{ini}-dependence in the present paper can be related to the energy dependence. In this limit, it is expected that many ordered states (in the onion structure) exist as distinct stable states, depending on the energy of the system. In this case our results imply that the degree of order decreases up to some energy, beyond which the order collapses.

Switching among ordered states through high-dimensional chaotic states have been extensively studied in dissipative systems, as chaotic itinerancy [27]. Switching between our clustered motions through random chaos provides an example of chaotic itinerancy in Hamiltonian systems. Similar ordered motion is seen in molecular dynamics simulations for glass [29] and water [30].

Both the dispersed and clustered states will hopefully be found in other physical systems, such as gravitational systems, microclusters of atoms, colloids, and so on. Phenomena which have been explained by stationary solutions so far may actually be ordered states sustained by chaotic motion as in our example.

Acknowledgements

We would like to thank Dr. Y.Aizawa, K. Ikeda, K. Shinjo, T. Yanagita, T. Ikegami, Y. Takahashi, S. Adachi, N. Gouda, S. Inagaki, Y-h. Taguchi, Y. Iba, and Y. Kikuchi for valuable discussions. T.K. thanks Prof. K. Nozaki and the members of R-lab. at Nagoya for useful discussions and encouragement. We are grateful to National Institute for Fusion Science at Nagoya for computational facility of FACOM VP200E, VP200 and M380. KK's research is partially supported by Grant-in-Aids for Scientific Research from the Ministry of Education, Science, and Culture of Japan.

References

[1] T. Konishi and K. Kaneko, J. Phys. A 25 (1992) 6283.
[2] T. Konishi and K. Kaneko, J. Phys. A 23 (1990) L715.
[3] R.S. MacKay and J. Meiss, eds., Hamiltonian Dynamical Systems (Adam Hilger, Bristol, 1987); A.J. Lichtenberg and M.A. Lieberman, Regular and Stochastic Motion (Springer, Berlin, 1983).
[4] B. V. Chirikov, Phys. Rep. 52 (1979) 263.
[5] V.I. Arnold, Sov. Math. Dokl. 5 (1964) 581. 4
[6] P.J. Holmes and J.E. Marsden, J. Math. Phys. 23 (1983) 669.
[7] N.N. Nekhoroshev, Russ. Math. Surv. 32 (1977) 1.
[8] M. Pettini and M. Landolfi, Phys. Rev. A 41 (1990) 768.
[9] D. Ruelle, Commun. Math. Phys. 87 (1982) 287.
[10] K. Kaneko, Collapse of Tori and Genesis of Chaos in Dissipative Systems (World Scientific, Singapore, 1986);
K. Kaneko, Simulating physics with coupled map lattices – pattern dynamics, information flow, and thermodynamics of spatiotemporal chaos, in: Formation, Dynamics, and Statistics of Patterns, K. Kawasaki, A. Onuki and M. Suzuki, eds. (World Scientific, Singapore, 1990) pp. 1–52, and references therein.
[11] C. Froeschlé, Astron. Astrophys. 16 (1972) 172.

[12] K. Kaneko and R.J. Bagley, Phys. Lett. A 110 (1985) 435.
[13] H-t. Kook and J. Meiss, Physica D 35 (1989) 65.
[14] H. Kantz and P. Grassberger, J. Phys. A 21 (1988) L127.
[15] K. Kaneko and T. Konishi, J. Phys. Soc. Jpn. 56 (1987) 2993.
[16] T. Konishi and K. Kaneko, in: Cooperative Dynamics in Complex Physical Systems, H. Takayama, ed. (Springer, Berlin, 1989).
[17] K. Kaneko and T. Konishi, Phys. Rev. A 40 (1989) 6130.
[18] T. Konishi, Prog. Theor. Phys. Suppl. 98 (1989) 19.
[19] Y. Aizawa et al., Prog. Theor. Phys. Suppl. 98 (1989) 36.
[20] N. Saito et al., J. Phys. Soc. Jpn. 27 (1969) 815.
[21] G. Benettin et al., C.R. Acad. Sci. Paris 286 (1978) A431.
[22] I. Shimada and T. Nagashima, Prog. Theor. Phys. 61 (1979) 1605.
[23] R.S. Ellis, Entropy, Large Deviation, and Statistical Mechanics (Springer, New York, 1985).
[24] Y. Kikuchi and Y. Aizawa, Prog Theor. Phys. 84 (1990) 1014.
[25] B.V. Chirikov and V.V. Vecheslavov, Theory of the Fast Arnold Diffusion in Many Frequency Systems (1992), Novosibirsk preprint 92-25.
[26] T. Musha, B. Gabor and M. Shoji, Phys Rev. Lett. 64 (1990) 2394.
[27] K. Kaneko, Physica D 41 (1990) 38;
K. Ikeda, K. Matsumoto and K. Ohtsuka, Prog. Theor. Phys. Suppl. 99 (1989) 295;
I. Tsuda, in: Neurocomputers and Attention, A.V. Holden and V.I. Kryukov, eds. (Manchester Univ. Press, Manchester, 1990).
[28] K. Kaneko, Physica D 54 (1991) 5.
[29] K. Shinjo, Phys. Rev. B 40 (1989) 9167.
[30] I. Ohmine and H. Tanaka, J. Chem. Phys. 93 (1990) 8138, and references therein.
[31] Jeffrey Tennyson, Physica D 5 (1982) 123.